Available online at www.sciencedirect.com
SCIENCE DIRECT®
Computational Materials Science 35 (2006) 216–222
COMPUTATIONAL MATERIALS SCIENCE
www.elsevier.com/locate/commatsci

# Growth dynamics of hydrogenated silicon nanoparticles under realistic conditions of a plasma reactor

H. Vach [a,*], Q. Brulin [a], N. Chaâbane [a], T. Novikova [a], P. Roca i Cabarrocas [a], B. Kalache [b], K. Hassouni [b], S. Botti [c], L. Reining [c]

[a] Laboratoire de Physique des Interfaces et des Couches Minces LPICM, UMR-7647 Ecole Polytechnique, 91128 Palaiseau Cedex, France
[b] Laboratoire d'Ingénierie des Matériaux et des Hautes Pressions LIMHP, Université de Paris 13, 93430 Villetaneuse, France
[c] Laboratoire des Solides Irradiés LSI, Ecole Polytechnique, 91128 Palaiseau Cedex, France

Received 24 April 2004; accepted 30 July 2004

**Abstract**

We present results of an extensive numerical study that was motivated by the experimental problem to understand under which conditions $Si_nH_m$ nanoparticles deposited by plasma enhanced chemical vapor deposition (PECVD) take an amorphous or a crystalline structure. A crystalline structure of those particles is crucial, for example, for the electrical properties and lifetime of polymorphous solar cells. First, we use a fluid dynamics model to characterize the experimentally employed silane plasma. The resulting relative densities for all plasma radicals, their temperatures, and their collision interval times are then used as input data for detailed semiempirical quantum molecular dynamics simulations. As a result the growth dynamics of nanometric hydrogenated silicon $Si_nH_m$ clusters is simulated starting out from the collision of individual $SiH_x$ radicals under the plasma conditions derived above. We demonstrate how the details of the plasma determine the amorphous or crystalline character of the forming nanoparticles. Finally, we show a preliminary absorption spectrum based on ab initio time-dependent DFT calculations for a crystalline $Si_{10}H_{16}$ cluster to demonstrate the possibility to monitor the cluster growth in situ.


*PACS:* 81.10.Bk; 61.46+w; 81.05.Zx; 81.07.Bc; 52.27.Lw

*Keywords:* Silicon; Hydrogen; Plasma; PECVD; Fluid dynamics model; Time-dependent DFT; Semiempirical molecular dynamics simulations; Cluster growth dynamics; Crystallization; Absorption spectrum; Nanostructures; Polymorphous silicon; Solar cells

## 1. Introduction

Polymorphous silicon is a nanostructured material consisting of a small fraction of nanocrystalline silicon particles or clusters embedded in a relaxed amorphous matrix. This heterogeneous material is produced under plasma conditions close to powder formation. The hydrogen bonding in this material was probed by infrared absorption and hydrogen evolution measurements. Surprisingly, the heterogeneous nature has no deleterious effect on the electronic and transport properties of these films; rather the transport and the hole transport in particular are better than those of standard amorphous silicon. These properties suggest polymorphous silicon be an excellent alternative to amorphous silicon [1].

Recently, it was demonstrated that those nanocrystalline silicon particles are actually produced in the gas phase of the plasma and *not* on the substrate itself [2]. However, no mechanism has yet been proposed to explain under which experimental conditions those nanoparticles take an amorphous or a crystalline structure.

* Corresponding author. Fax: +33 1 69 33 30 06.
*E-mail address:* vach@leonardo.polytechnique.fr (H. Vach).

0927-0256/$ - see front matter © 2005 Elsevier B.V. All rights reserved.
doi:10.1016/j.commatsci.2004.07.010

In the following, we will therefore present a semiempirical quantum molecular dynamics simulation of the growth dynamics of nanometric hydrogenated silicon particles in the gas phase of a plasma reactor.

In Section 2, we will characterize the employed plasma by means of a fluid dynamics model. Then, we will investigate the cluster growth under two different experimental conditions using semiempirical quantum molecular dynamics. In Section 4, we will then show our first result of an absorption spectrum obtained with a time-dependent DFT approach.

## 2. Fluid dynamics model calculations of the plasma

### 2.1. Model description

A glow discharge plasma is obtained by coupling electric power to a neutral background gas. Basically, the electric energy coupled to the system allows for ionization of the neutral gas which is subsequently sustained by ionizing electron-impact collisions. Besides the ionization reactions leading to positive ions and electrons, a variety of inelastic electron collisions also produce radicals and negative ions through attachment reactions for instance. Those heavy species, namely ions and radicals formed by primary reactions can react through secondary reactions including polymerization reactions, giving rise to a complex chemistry at the origin of the nanoparticles formation. Therefore, plasma parameters such as the species (electrons, ions and radicals) density and energy, are the basis of any nanoparticle growth simulation if realistic simulations describing real operating discharge conditions, is intended. For this purpose, we make use of a plasma model.

Our plasma model deals with a conventional radio frequency (13.56 MHz), parallel plate, capacitively coupled glow discharge. The discharge is operated in a $SiH_4$/$H_2$ mixture, the considered pressure range lies between 0.25 and 2.00 Torr, and the RF voltage is varied between 100 and 500 V. A 1D model is used as we are interested in the plasma chemistry rather than specific geometry effects. Using a 2D model would have increased the computational time without any qualitative improvement of the resulting predictions. The plasma is described by a set of 12 species including the background gas ($H_2$, $SiH_4$), radicals (H, $SiH_2$, $SiH_3$), positive and negative ions ($H^+$, $H^-$, $H_2^+$, $H_3^+$, $SiH_2^+$, $SiH_3^+$, $SiH_3^-$) and electrons, interacting through a set of 38 chemical reactions. The transport dynamics of the species is treated within the assumption of the hydrodynamics regime also referred to as the fluid approximation. The fluid approximation holds if the species mean free path $\lambda$ is much smaller than the characteristic gradient lengths ($\lambda \nabla n/n \ll 1$), a condition which is fully satisfied in our operating discharge conditions. The fluid model equations are based on the density continuity equation and the momentum continuity equation of both charged species and neutrals, and the energy continuity equation of the electrons. Details on the model equations and the numerical algorithms can be found in Ref. [3]. Basically, our code allows for calculating the species density and energy profiles across the discharge as well as the electric potential profile.

### 2.2. Typical results

Fig. 1 shows the time-averaged electric potential profile across the discharge. Typically, the profile consists of a flat potential region corresponding to the plasma bulk where the electric field is almost zero and two potential drop regions, the so-called plasma sheaths. Basically, this feature of the potential profile reflects the response of the plasma to the excitation electric field for preserving its macroscopic electric neutrality. The ion energy profiles of $SiH_3^+$ and $SiH_2^+$ are shown in Fig. 2. Ions are in thermal equilibrium with the room temperature background gas in the plasma bulk, and might only gain energy as they are accelerated by the sheath potential.

Typical results of a simulation carried out at a typical experimental pressure of 1 Torr, an RF voltage of 300 V, and a 2% $SiH_4$ in $H_2$ mixture, are presented here. Time-averaged density profiles of the most important radicals and silane ions (H, $SiH_2$, $SiH_3$, $SiH_2^+$, $SiH_3^+$) are plotted in Fig. 3. This figure shows that H and $SiH_3$ are the major plasma species in agreement with previous experimental observations made in this range of operating discharge parameters [4]. The density profiles result from a competition between the gas-volume chemical reactions source terms and transport terms. For the molecular dynamics simulation of below, we like to point out, however, that the densities displayed in Fig. 3 only concern species created by the plasma discharge and not the background $SiH_4$ molecules: while $SiH_3$ is clearly the most abundant plasma created

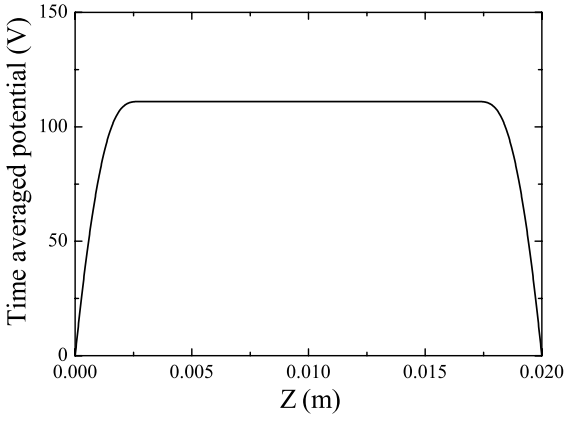


Fig. 1. Time-averaged electric potential profile.

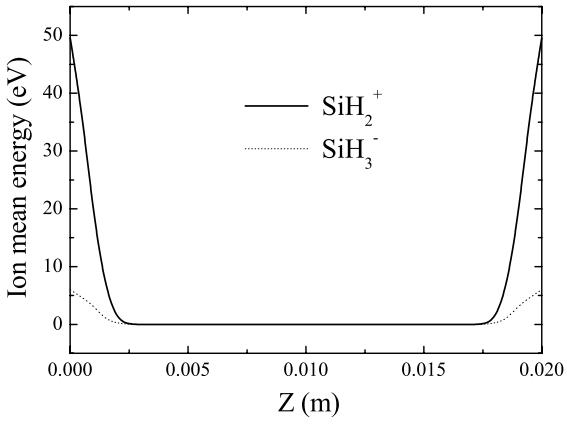


Fig. 2. Time-averaged ion mean energy profiles.

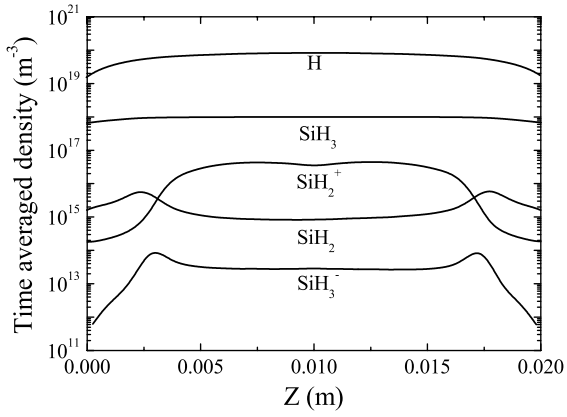


Fig. 3. Time-averaged species density profiles.

species, the density of background $SiH_4$ molecules is still roughly 1000 times higher.

## 3. Molecular dynamics simulations of the cluster growth

Minimum energy structures have previously been calculated for both pure silicon clusters [5] and hydrogenated silicon clusters [6]. The experimental observation of powder formation in the plasma shows, however, that the dominantly formed particles do not necessarily correspond to those global minimum energy structures. Therefore, it appears to be mandatory to simulate the cluster growth *dynamics* under realistic plasma conditions. In the previous section, we derived the relative density of each plasma species. We also showed that those plasma species are in thermal equilibrium with the room temperature $SiH_4$ background gas. In the present section, we will use this information as input data for our detailed molecular dynamics study. First, we will demonstrate the validity of our semiempirical quantum approach in comparison with high-level ab initio calculations and experimental cross section measurements. Then, we study the most important energy transfer channels involved in the reactive scattering of silicon ions with vibrationally and rotationally excited hydrogen molecules. The respective roles played by initial vibrational and rotational excitation of the reactants for the reactivity enhancement of the silicon/hydrogen system are investigated. Finally, we use the same simulation approach to explore the details of the cluster growth dynamics.

### 3.1. Simulation approach

Our recent experimental observation that the $Si_nH_m$ clusters grow in the gas phase and not on the substrate permits us to use quantum molecular dynamics simulation QMDS to study the cluster growth mechanisms in the plasma. Above, we determined the relative densities of all $SiH_x$ radicals, their charge states, their kinetic energies, collision intervals, and vibrational temperatures necessary for the initial conditions of our semiempirical quantum molecular dynamics simulations. Many interatomic model potentials have been developed that permit direct calculation of the structural dynamics of complex semiconductors systems [7,8]. The use of those model potentials gives detailed information on the dynamics of the studied systems [9]. However, those studies strongly rely on the used model potentials and on the employed switching functions. Using density functional theory, on the other hand, Muller et al. thoroughly analyzed the energetics and rates of possible gas-phase reactions between Si and $SiH_4$ without the use of any model potentials [10]. While their outstanding work has direct implications for hot-wire chemical vapor deposition, it does not give detailed information on the underlying reaction dynamics.

In the present paper, we performed trajectory calculations where all necessary interatomic potentials were determined *"on the fly"* using quantum chemistry. In this manner, we obtained time resolved information on the reaction dynamics without using model potentials or switching functions. Due to the enormous computational costs of ab initio calculations with appropriate basis sets, we employed semiempirical PM3 quantum calculations and we showed that we can not only reproduce all of the experimental results of Armentrout [11], but that we also obtain a much more detailed insight in the underlying elementary reaction dynamics not accessible to previous experiments or simulations (see Fig. 4 and Ref. [12]).

### 3.2. Energy transfer mechanisms

The fluid model described above relays on the knowledge of energy dependent reactive cross sections for the correct implementation of the 38 considered chemical reaction. In Fig. 5, we showed the dependence of one of the most important primary reactions on kinetic

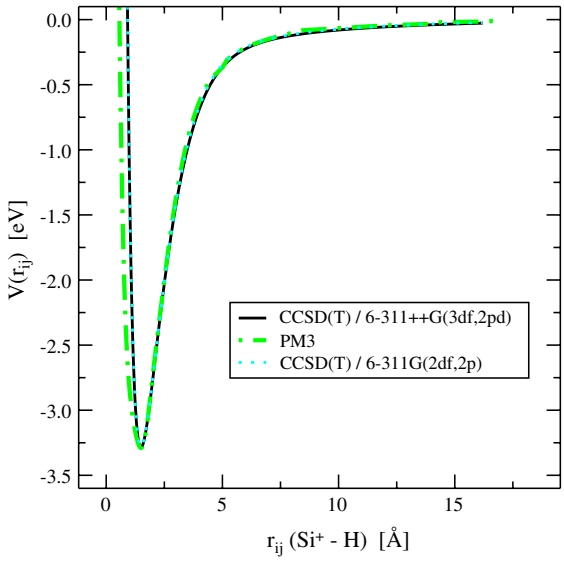


Fig. 4. Potential energy curve for the $SiH^+$ molecule calculated with the semiempirical PM3 method in comparison to high-level ab initio CCSD(T) calculations.

impact energy. In the following, we investigate the influence of *internal* reactant energy; i.e., we investigate the details of energy flow between the different degrees of freedom during the reactive scattering of $Si^+$ with $H_2(v_0, J_0)$ [13]. Notably, we demonstrate that excitation of the internal reactant energy can lead to a considerable enhancement of reactivity (compare Figs. 5 and 6). In addition, we show that both the absolute amplitude of the reactive cross section and the shift of its maximum toward lower impact energies only depend on the *amount* of initial internal excitation and not on its precise *nature*; i.e., initial *rotational* excitation enhances the reactivity of our system in the same way as prior *vibrational* excitation (see Fig. 6).

We also showed that there are always two reaction channels: a direct one and an intermediate complex-mediated one. It is the lifetime of this intermediate complex that determines the maximum vibrational energy the SiH products can obtain during the reactive scattering event (see Fig. 7 and Ref. [13] for more details).

### 3.3. Cluster growth dynamics

Based on our fluid model calculations of above, we know that our silane plasma can essentially be described by mainly $SiH_4$ molecules and a small fraction of $SiH_3$ radicals. Since the reaction probability between two $SiH_4$ molecules is quite negligible at our room temperature conditions, cluster growth can only start once a $SiH_4$ molecule encounters a $SiH_3$ radical.

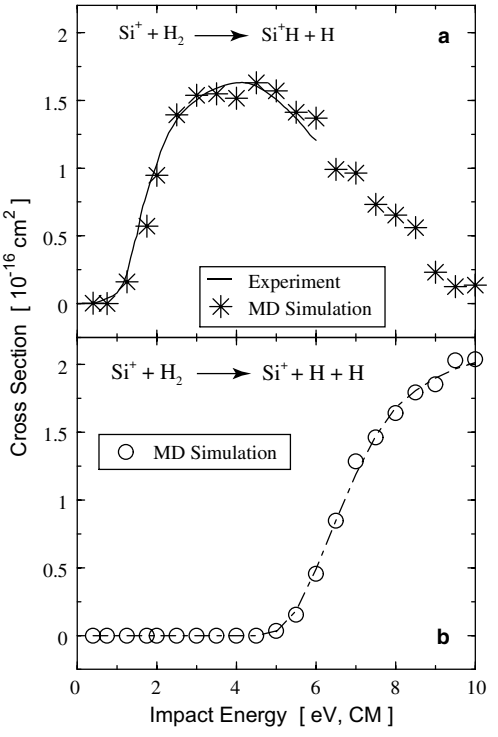


Fig. 5. Calculated and measured reaction cross sections $\sigma$ as function of relative impact kinetic energy (a) for $SiH^+$ production and (b) for complete dissociation.

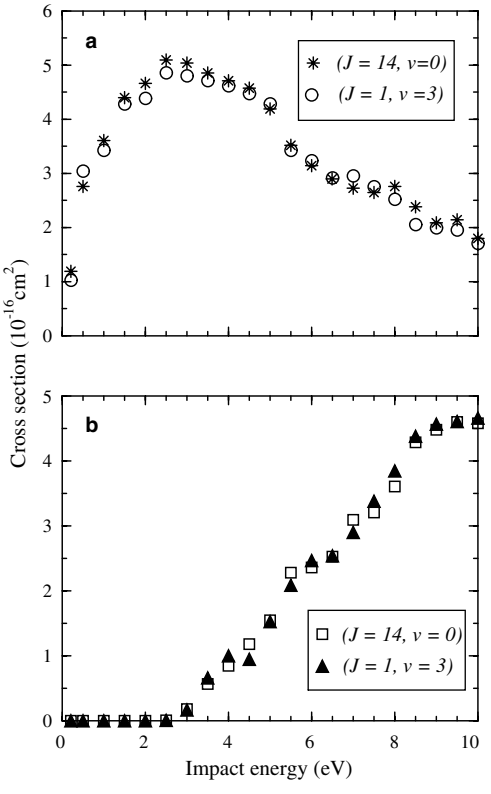


Fig. 6. Calculated reaction cross sections $\sigma$ as function of relative impact kinetic energy for an initial laser excitation of the $H_2$ reactant to ($v_0 = 3$, $J_0 = 1$) and ($v_0 = 0$, $J_0 = 14$) both corresponding to an internal energy $E_{int}$ of 1.8 eV. (a) For $SiH^+$ production: $Si^+ + H_2(v_0, J_0) \rightarrow SiH^+(v, J) + H$ and (b) for complete dissociation: $Si^+ + H_2(v_0, J_0) \rightarrow Si^+ + H + H$.

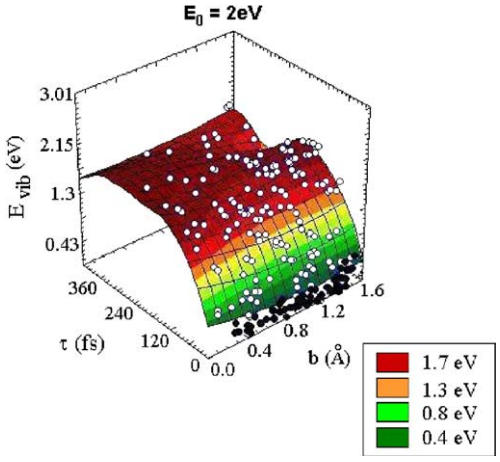


Fig. 7. Correlation between $SiH^+$ vibrational energy $E_{vib}$, impact parameter $b$ and $SiH_2$ complex lifetimes $\tau$ for $SiH^+$ products.

After this first reaction, the impact of additional $SiH_4$ molecules is sufficient to ensure the continuation of the cluster growth. In this manner, we followed the growth dynamics up to $Si_nH_m$ clusters of nanometric size using the same semiempirical quantum molecular dynamics approach as above (see Fig. 8). The hydrogen atoms always remain at the surface of the forming hydrogenated silicon clusters. Directly after the impact of a new molecule, those hydrogen molecules easily "jump" from one dangling bond to another.

In Fig. 9, we displayed the typical geometry of a nanometric $Si_{27}H_{25}$ cluster. As all clusters that we grew under our present room temperature plasma conditions, this cluster shows an amorphous structure.

To gain a deeper insight in the growth mechanism, we then studied the cluster growth for $SiH_4$ molecules impacting with an energy of 2.0 eV. Three typical results are shown in Fig. 10. A general finding is that the

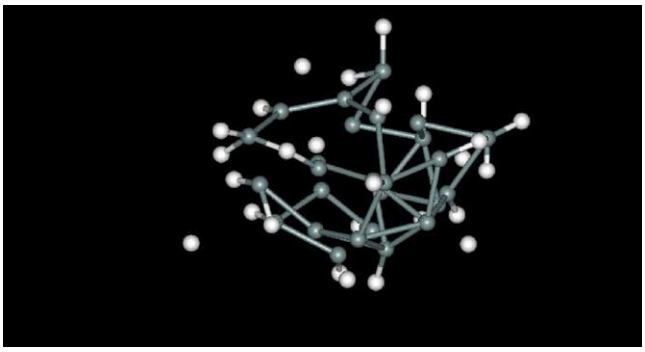

Fig. 9. A typical geometrical structure obtained for the growth of a $Si_{27}H_{25}$ cluster considering thermal impact energies of the plasma species.

contents of hydrogen in the final clusters is now considerably lower than for the room temperature case. Yet more striking, however, is the observation that the clusters now crystallize in structures that are very comparable to those predicted for pure $Si_n$ clusters by Raghavachari [14]. In Fig. 11, we show two typical radial distribution functions as obtained from clusters grown with two different impact energies. Since the higher impact energy clearly facilitates the growth of crystalline silicon structures, we suggest that plasmas of higher temperature might be potentially interesting for the growth of crystalline nanostructure.

## 4. Time-dependent DFT calculations for the cluster absorption spectrum

We have calculated a preliminary optical absorption spectrum for a spherical cluster $Si_{10}H_{16}$ with a diameter of 0.8 nm (see Fig. 12). The geometry of this cluster is obtained by cutting a spherical portion of the perfect

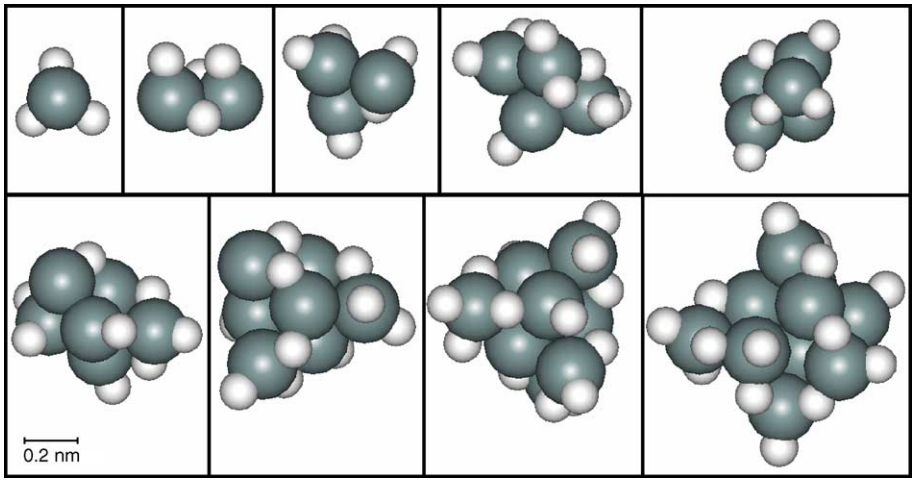


Fig. 8. Typical geometrical structures obtained from a cluster growth under realistic plasma conditions. We like to point out that the hydrogen atoms always remain at the outside of the $Si_nH_m$ clusters.

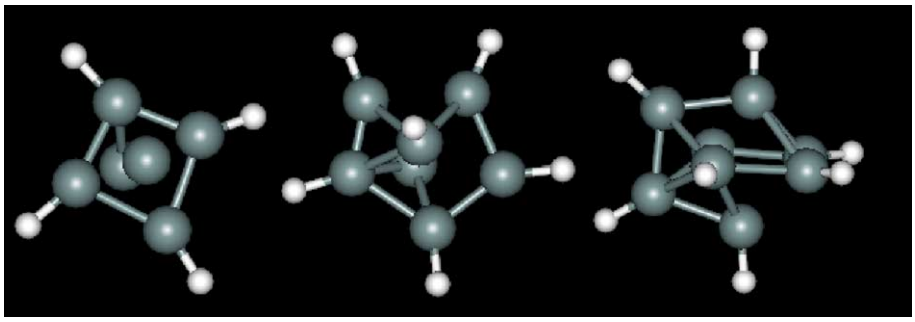

Fig. 10. Typical geometrical structures obtained for the growth of $Si_nH_m$ clusters considering impact energies of 2 eV.

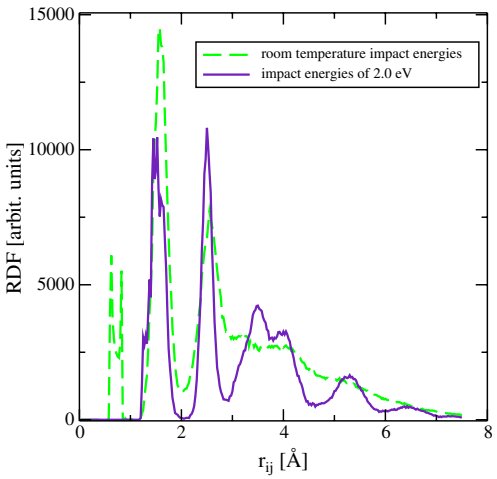


Fig. 11. Radial distribution functions for two typical $Si_{10}H_m$ clusters obtained for two different impact energies for the colliding plasma species (see text).

Si crystal and then saturating the dangling bonds with hydrogen atoms oriented in the direction of the missing bonds. A structural relaxation was performed before proceeding with the calculation of the spectrum. Important effects on the peak positions are dependent on the cluster size. As a general rule, when the cluster size decreases, the increase in the quasiparticle gap blue shifts the absorption edge, while the increase in the excitonic binding energy red shifts the edge. Both effects have to be correctly accounted for to obtain an accurate description of the optical spectra. To this purpose, we calculated electronic excitations within time-dependent density functional theory (TDDFT) [15,16], using a real-space, real-time approach to solve the time-dependent Kohn–Sham equations, implemented in OCTOPUS [17]. This approach has widely proved in the last years to provide an accurate description of optical properties of nanostructured materials [18]. The electron–ion interaction is described through norm-conserving pseudo-potentials [19] and exchange–correlation terms are included in the local density approximation (LDA). Calculations are performed at zero temperature and fixed geometry. An uniform grid spacing of 0.25 Å and a time step of 0.004 fs assures a stable propagation and a peak resolution better than 0.1 eV.

To calculate the dipole strength function (which is proportional to the absorption cross section) we excite the system from its ground state by applying a delta electric field $E_0\delta(t)$. In Fig. 13, we demonstrate the cluster response in the $t \to \infty$ approximation exhibiting a series

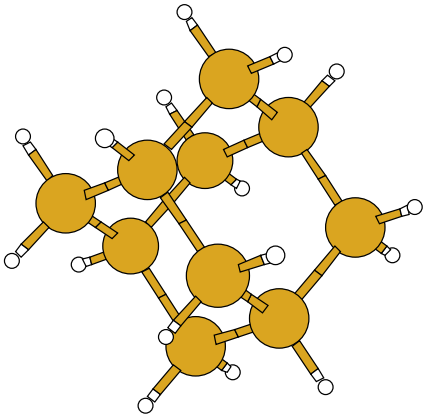

Fig. 12. Geometrical structure of the considered $Si_{10}H_{16}$ cluster.

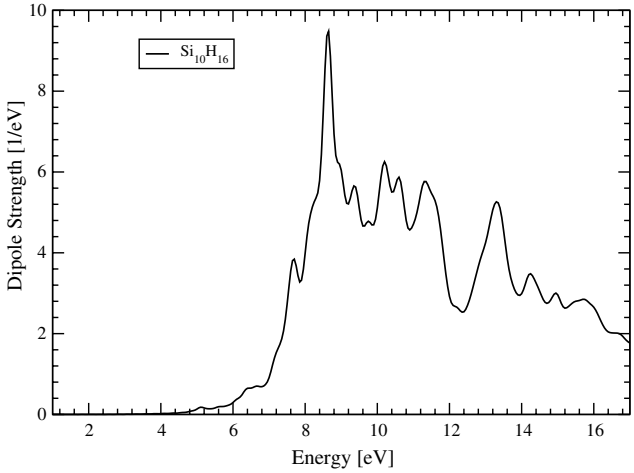


Fig. 13. Calculated averaged dipole strength for $Si_{10}H_{16}$.

of sharp peaks in the 7–16 eV range. Finally, we like to mention that calculations for spectra of silicon hydrogenated systems have previously been performed using GGA exchange and correlation functionals. Those spectra are practically identical to our LDA spectra, as can be seen in the work by Marques et al. [20].

## 5. Conclusion

Our present work was stimulated by the experimental problem to understand the mechanisms leading to the formation of crystalline or amorphous hydrogenated silicon clusters in a plasma discharge. Employing a fluid dynamics model, we derived the relative densities and temperatures of all species present in a typical silane plasma. By means of semiempirical quantum molecular dynamics, we then investigated the dynamics of the cluster growth based on our results obtained from the fluid model. We demonstrated that the final cluster structure strongly depends on the details of the plasma parameters. Notably, we suggest that the use of hotter silane plasmas should favor the formation of crystalline cluster structures. Finally, we calculated the optical absorption spectrum of one of those hydrogenated silicon clusters using time-dependent density functional theory. In the future, we will use the resulting absorption spectra in the IR and UV to monitor the cluster growth in situ experimentally.

## References

[1] P. Roca i Cabarrocas, A. Fontcuberta i Morral, Y. Poissant, Thin Solid Films 403 (2002) 39.
[2] N. Chaâbane, A.V. Kharchenko, H. Vach, P. Roca i Cabarrocas, New J. Phys. 5 (2003) 1.
[3] T. Novikova, B. Kalache, P. Bulkin, K. Hassouni, W. Morscheidt, P. Roca i Cabarrocas, J. Appl. Phys. 93 (2003) 3198.
[4] O. Leroy, G. Gousset, L.L. Alves, J. Perrin, J. Jolly, Plasma Sources Sci. Technol. 7 (1998) 348.
[5] U. Röthlisberger, W. Andreoni, M. Parrinello, Phys. Rev. Lett. 72 (1994) 665.
[6] G. Onida, W. Andreoni, Chem. Phys. Lett. 243 (1995) 183.
[7] F. Stillinger, T. Weber, Phys. Rev. B 31 (1985) 5262.
[8] J. Tersoff, Phys. Rev. Lett. 56 (1986) 632.
[9] S. Ramalingam, S. Sriraman, E.S. Aydil, D. Maroudas, Appl. Phys. Lett. 78 (2001) 2685.
[10] R.P. Muller, J.K. Holt, D.G. Goodwin, W.A. Goddard III, Mat. Res. Soc. Symp. Proc. 609 (2000) A6.1.1.
[11] J.L. Elkind, P.B. Armentrout, J. Phys. Chem. 88 (1984) 5454.
[12] H. Vach, N. Chaâbane, G.H. Peslherbe, Chem. Phys. Lett. 352 (2002) 127.
[13] N. Chaâbane, H. Vach, P. Roca i Cabarrocas, J. Phys. Chem. A 108 (2004) 12.
[14] K. Raghavachari, J. Chem. Phys. 84 (1986) 5672.
[15] E.K.U. Gross, W. Kohn, Phys. Rev. Lett. 55 (1985) 2850.
[16] E.K.U. Gross, W. Kohn, Phys. Rev. Lett. 57 (1986) 923.
[17] M.A.L. Marques, A. Castro, G.F. Bertsch, A. Rubio, Comput. Phys. Commun. 60 (2003) 151. Available from: <www.tddft.org/programs/octopus>.
[18] G. Onida, L. Reining, A. Rubio, Rev. Mod. Phys. 74 (2002) 601, and references therein.
[19] D.R. Hamann, M. Schlüter, C. Chiang, Phys. Rev. Lett. 43 (1979) 1494.
[20] M.A.L. Marques et al., J. Chem. Phys. 115 (2001) 3006.